Rationale, Design, and Synthesis of Novel Phenyl Imidazoles as Opioid Receptor Agonists for Gastrointestinal Disorders

Henry J. Breslin,* Tamara A. Miskowski, Bryan M. Rafferty, Santosh V. Coutinho, Jeffrey M. Palmer, Nathaniel H. Wallace, Craig R. Schneider, Edward S. Kimball, Sui-Po Zhang, Jian Li, Raymond W. Colburn, Dennis J. Stone, Rebecca P. Martinez, and Wei He

Johnson & Johnson Pharmaceutical Research & Development, L.L.C., Welsh and McKean Roads, P.O. Box 776, Spring House, Pennsylvania 19477-0776

Received October 28, 2003

A small series of novel, imidazoles **4** have been prepared that exhibit very good binding affinities for the δ and μ opioid receptors (ORs), as well as demonstrate potent agonist functional activity at the δ OR. Representative imidazole **4a** (K_i δ = 0.9 nM; K_i μ = 55 nM; K_i κ = 124 nM; EC_{50} δ =13−25 nM) was further profiled for OR related in vivo effects. Compound **4a** reduced gastrointestinal (GI) propulsive motility in a dose-dependent and naloxone-reversible manner, based on the results of the mouse glass bead expulsion test (3, 5, and 10 mg/kg, ip) and the mouse fecal pellet output test (1 and 3 mg/kg, ip). Compound **4a** showed no analgesic activity as measured by the mouse abdominal irritant test (MAIT) when dosed at 100 mg/kg, sc, but did show significant MAIT activity at doses of both 10 μg (40% inhibition) and 100 μg (100% inhibition) when dosed intracerebroventricularly (icv). Taken together, these in vivo results suggest that **4a** acts peripherally when dosed systemically, and that these prototypical compounds may prove promising as medicinal leads for GI indications.

Introduction

Compounds that modulate opioid receptors (ORs) are well recognized as being useful therapeutic agents for pain management (e.g., morphine;[1] fentanyl;[1] Figure 1), and gastrointestinal (GI) motility regulation (e.g., loperamide;[1] Figure 1). These opioid therapeutic effects and other opioid-mediated pharmacological observations were relatively well categorized long before the molecular biology of opioids was understood and were largely tied to the specific class of opioids known as opiates.[1] A molecular mechanism of action for the observed opioid pharmacology was determined more recently when the G-protein-coupled ORs were discovered in the 1970s. The ORs were quickly categorized into three subsets of receptors (δ, μ, and κ), which more recently were further subdivided pharmacologically into multiple subtypes. Subsequent OR studies have documented pharmacological and functional interactions between the μ and δ ORs and suggest that modulation of both receptors simultaneously may be beneficial.[2] It has also recently been postulated that compounds that preferentially target the peripheral δ OR may provide therapeutic benefit in gastrointestinal disorders, while circumventing central μ opioid receptor related side effects.[2]

Soon after the ORs were characterized, the pentapeptide enkephalins were identified as a set of endogenous OR ligands (e.g.: Tyr-Gly-Gly-Phe-Leu).[3] Since the discovery of the enkephalins, many groups have explored modifying the parent pentapeptides, yielding little success in identifying useful medicinal agents. One approach explored has been the truncation of the enkephalin pentapeptides. An initial truncation of the enkephalins led to a set of modified tetrapeptides that maintain comparable OR affinities to the enkephalins [e.g.: Tyr-Tic-Phe-Phe (TIPP; **1a**); Scheme 1].[4] The modified tetrapeptides were subsequently further truncated to a set of modified dipeptides, which exhibit very good δ OR agonist activities (e.g.: **1b**; Scheme 1).[5] Besides their potential medicinal value, these truncated enkephalin analogues began to clarify key chemical and conformational features of the enkephalins required for favorable OR binding activity.[6] Although these truncated analogues can be viewed as an advancement toward the design and discovery of new opioids, one potential drawback noted for some of the truncated compounds is their inherent instability potential to cyclize on themselves, extruding an amine **3** while concurrently forming the considerably less active[7] diketopiperazine ring **2** (Scheme 1).

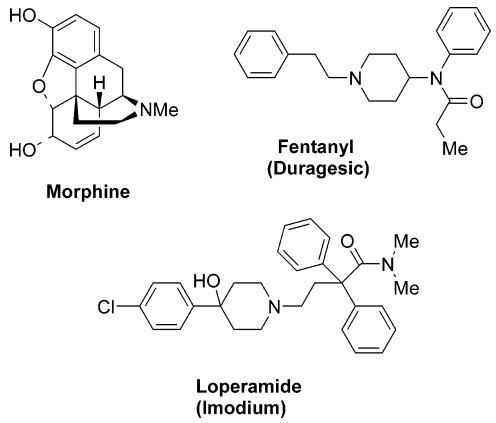

Figure 1. Historical opioid receptor agonists.

Recently we modified a previously reported cholecystokinin (CCK)-related dipeptide (**1c**;[8] Scheme 1) that has an identical diketopiperazine cyclization liability[9] (**2c**; Scheme 1) as noted for the truncated enkephalins.

* To whom correspondence should be addressed. Fax: (215) 628-4985. E-mail: HBreslin@prdus.jnj.com.

10.1021/jm030548r CCC: $27.50
Published on Web 09/04/2004

Scheme 1

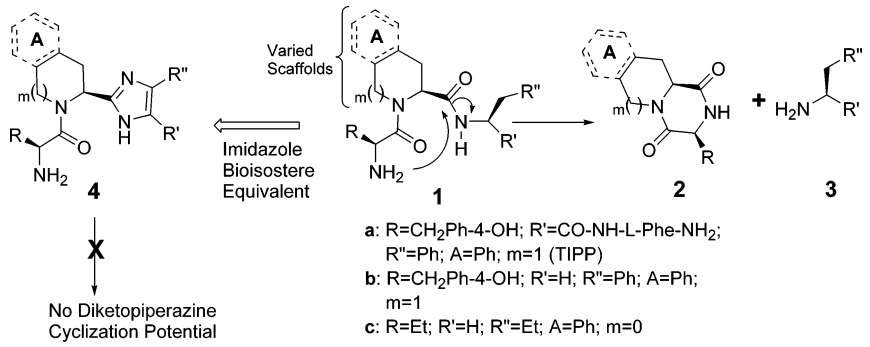

Table 1. Final Target Compounds **4** and **5**

no.	R	R′	R″	A	*m*
4a	CH_2-Ph-4-OH	H	Ph	fused Ph	1
4b	Et	H	n-Pr	fused Ph	0
4c	CH_2-Ph-4-OH	Me	Ph	fused Ph	1
4d	CH_2-Ph-4-OH	Br	Ph	fused Ph	1
4e	CH_2-Ph-4-OH	Me	n-Pr	fused Ph	1
4f	CH_2-Ph-4-OH	fused Ph (i.e. benzimidazole)		fused Ph	1
4g[a]	CH_2-2,6-di-Me-Ph-4-OH	fused Ph (i.e. benzimidazole)		fused Ph	1
4h	CH_2-Ph-4-OH	Me	Ph	−	1
4i	CH_2-Ph-4-OH	Me	Ph	−	0
5a	CH_2-Ph-4-OH	Me	Ph	fused Ph	1
5b	CH_2-Ph-4-OH	Me	n-Pr	fused Ph	1
5c	CH_2-Ph-4-OH	fused Ph (i.e. benzimidazole)		fused Ph	1

[a] Previously reported compound.[14]

Except for the potential cyclization liability, the CCK related dipeptides are structurally distinct from the opioids, possessing a different scaffold (indoline for **1c**; tetrahydroisoquinoline for **1a**,**b**) and different appendages (i.e. R, R′, and R″). For the CCK series of compounds, we substituted an imidazole moiety (e.g.: **4b**;[9] Table 1) as a bioisostere for the susceptible amide moiety of **1c** and experimentally demonstrated that we could circumvent the diketopiperazine cyclization liability noted for the amide series. We also demonstrated that these related imidazoles and amides maintained similar H bonding potentials and good conformational overlap, based on molecular modeling calculations. Most significant was our experimental finding of identical biological activities for the imidazoles as for the parent amide structures.

Noting the similar chemical liabilities between the CCK analogue **1c** and enkephalin amides **1a/1b**, we questioned whether our earlier CCK findings could be extrapolated to the structurally dissimilar truncated enkephalins (Scheme 1). If successful, this extrapolation would yield potent imidazole-opioid compounds **4** (Scheme 1) with improved inherent stability over their parent amides **1**, as well as additional stability against potential protease degradation. Another potential benefit of imidazoles **4**, if they retained good OR activities, would be the added insight for the conformational pharmacophore requirements for OR ligands. This postulate was proposed as a promising possibility since imidazole **4** has three additionally constrained bonds when overlaid on the freely rotating amide appendage of **1**; thus, **4** has considerably fewer degrees of freedom than **1**. Finally, and most importantly, we wanted to assess the in vivo profile of these novel imidazole structures **4**, should they demonstrate favorable in vitro OR activity.

Based on these above rationales and questions, synthetic efforts were initiated toward imidazole-opioids **4**. Following are described our initial experimental results for the preparation and activities of **4**.

Chemistry

Novel imidazoles **4** were prepared via one of two routes. The stereospecific preparation of disubstituted imidazole **4a** (Scheme 2) was begun with a high yielding 1-[3-(dimethylamino)propyl]-3-ethylcarbodiimide/1-hydroxybenzotriazole (EDC/HOBT) amide coupling reaction between commercial reagents **6a** and **7a**, to generate **8a**. Amide **8a** was converted to imidazole **9a** in modest yield following an imidazole ring-forming procedure,[10] by warming **8a** with ammonium acetate (NH_4-OAc) in acetic acid (AcOH). The *tert*-butoxycarbonyl (t-BOC) protecting group of **9a** was readily cleaved with trifluoroacetic acid (TFA) at 0 °C to give **10a**. Crude **10a** was reacted directly with an in situ-generated isobutyl chloroformate mixed anhydride of commercially available N-t-BOC-O-*tert*-butyl-L-tyrosine (BOC-Tyr(*t*Bu)-OH), with a good overall two-step yield for **11a**. Noteworthy is that this stereospecific route was epimerization free after these four initial steps, with **11a** proving to be a pure compound as determined by high-pressure liquid chromatography (HPLC) and thin-layer chromatography (TLC). Treatment of **11a** with TFA at 0 °C quickly removed both the N-BOC and O-t-Bu protecting groups to give initial target compound **4a**. Intermediate **11a** was alternatively treated with bromine (Br_2) in chloroform ($CHCl_3$) at 0 °C to generate 5-bromo-imidazole **11d** in good yield. Intermediate **11d** was also readily di-deprotected with TFA leading to the isolation of product **4d**. The synthetic sequence of Scheme 2 also proved fruitful in the preparation of trisubstituted imidazoles **4h** and **4i**. A couple of variances were incorporated into the scheme for piperidine **4h** and pyrrolidine **4i**, based on knowledge gained in the preparation of **4a**. We had found that the imidazole ring-forming cyclization of **8a** had resulted in a modest return of **9a** at best. We assumed that the modest yield might be in part a result of some instability of the acid sensitive BOC protecting group of starting material **8a**, and/or of product **9a**, under the somewhat harsh acidic reaction conditions (AcOH warmed to 100 °C). On the basis of this hypothesis, we altered the nitrogen-protecting group in our followup piperidine and pyrrolidine sequences to the more acid stable benzyloxycarbonyl (CBZ) protecting group. We also altered our

Scheme 2

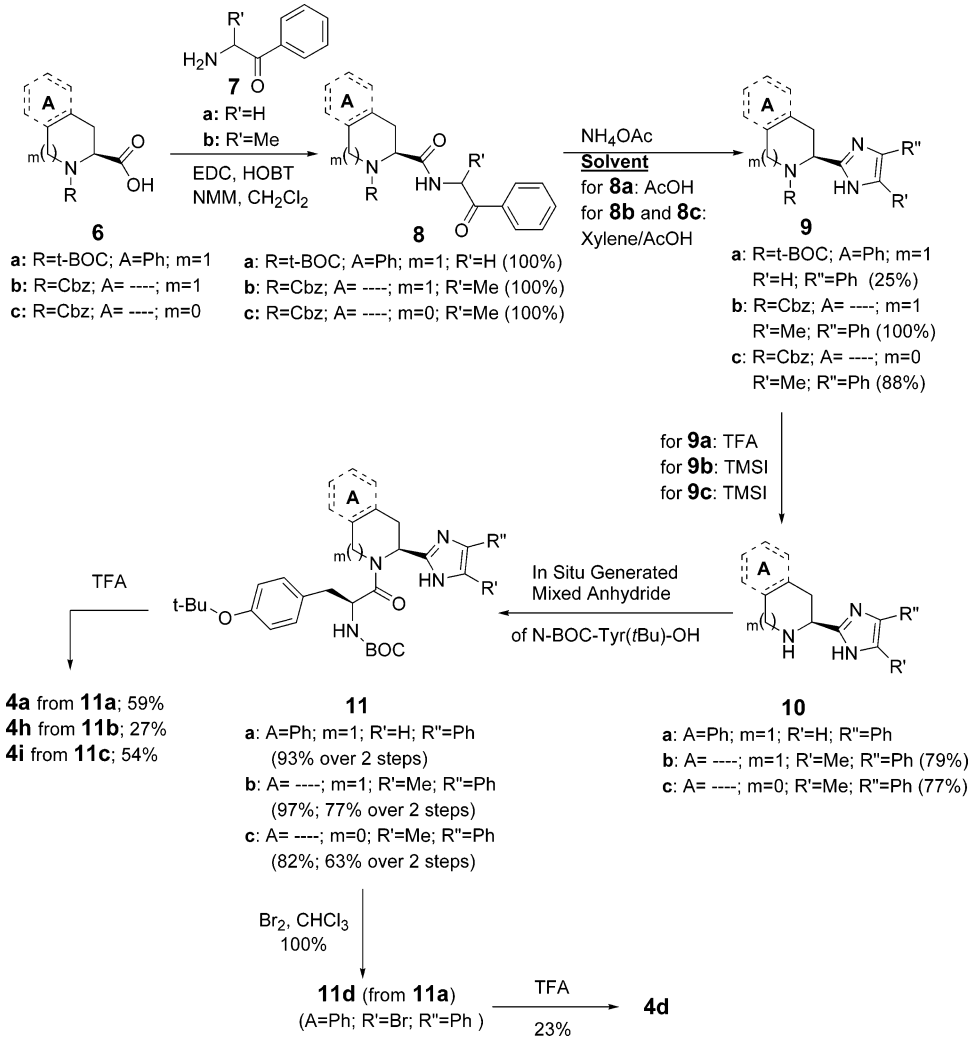

solvent for the imidazole ring forming reaction to a mixed solvent system of refluxing xylene/AcOH, which has been reported in the literature as being favorable for such cyclizations.[11] Following these alternate reaction conditions, we obtained improved yields of imidazoles **9b** and **9c**. Subsequently we easily removed the CBZ protecting groups of **9b** and **9c** with iodotrimethylsilane (TMSI) to give nor-amines **10b** and **10c**, respectively. Amines **10b** and **10c** were carried on through the remainder of the sequence in a similar manner as described above for **10a**, ultimately yielding respective desired target **4h** and **4i**.

Another sequence explored in generating trisubstituted imidazoles **4c** and **4e** is outlined in Scheme 3. The previously reported aldehyde **12**[12] was reacted with commercially available diketones **13** under Radziszewski reaction[13] conditions to generate the desired trisubstituted imidazole intermediates **9d** and **9e** in reasonable yield. As in our prior sequence, intermediates **9d** and **9e** were readily deprotected with TFA at 0 °C to yield amines **10d** and **10e**, respectively. Coupling of these amines with the in situ generated isobutyl chloroformate mixed anhydride of BOC-Tyr(*t*Bu)-OH led to desired products **11**. However, we were disappointed to find that with this synthetic route a mixture of epimers (**11** and **14**) were observed by HPLC/MS for both amines during this coupling step. This discrepancy between Schemes 2 and 3 suggests that the partial isomerization for Scheme 3 likely occurs during the heterocyclic ring forming reaction to generate imidazoles **9**. Fortunately, separation of both sets of epimers from Scheme 3 proved cooperative via preparative HPLC, i.e. separation of **14a** from **11e** and **14b** from **11f**, respectively. The resulting sets of pure compounds were easily deprotected with TFA, as already mentioned for similar adducts discussed in Scheme 2. Although Scheme 3 proved generally unattractive due to the noted partial epimerizations, we did benefit from this synthetic effort since it yielded the ready opportunity of measuring relative biological activities for respective epimers **4c** with **5a** and **4e** with **5b**.

Benzimidazole targets **4f** and **5c** were prepared as depicted in Scheme 4. Acid **6d** was cleanly coupled with 1,2-phenylenediamine via a standard EDC/HOBT amide coupling reaction to give amide **15**. Compound **15** was internally cyclized and dehydrated in warm AcOH, generating benzimidazole intermediate **9f** in good yield. Unfortunately, complete epimerization of the chiral center of compound **15** occurred during this cyclization, as determined by chiral chromatography. Similar to our earlier examples, TMSI efficiently removed the CBZ protecting group of **9f** to yield noramine **10f**. Noramine **10f** was coupled with BOC-Tyr(*t*Bu)-OH via an EDC/HOBT amide coupling reaction. The resulting crude

Scheme 3

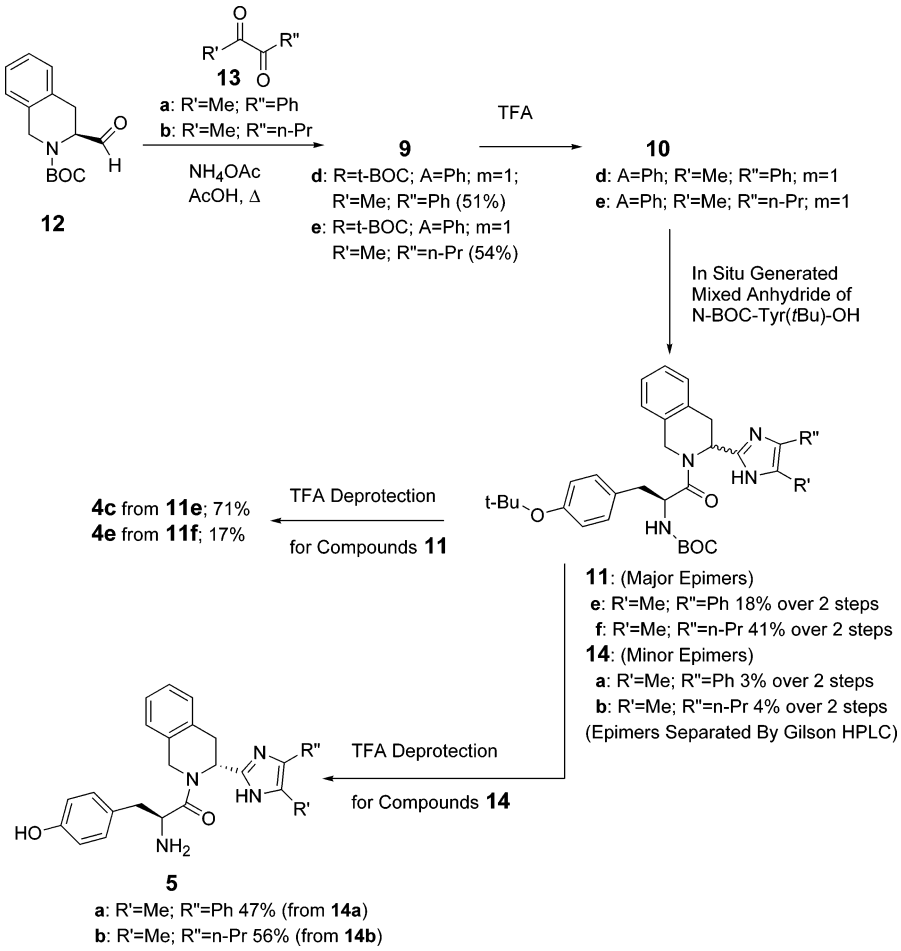

Scheme 4

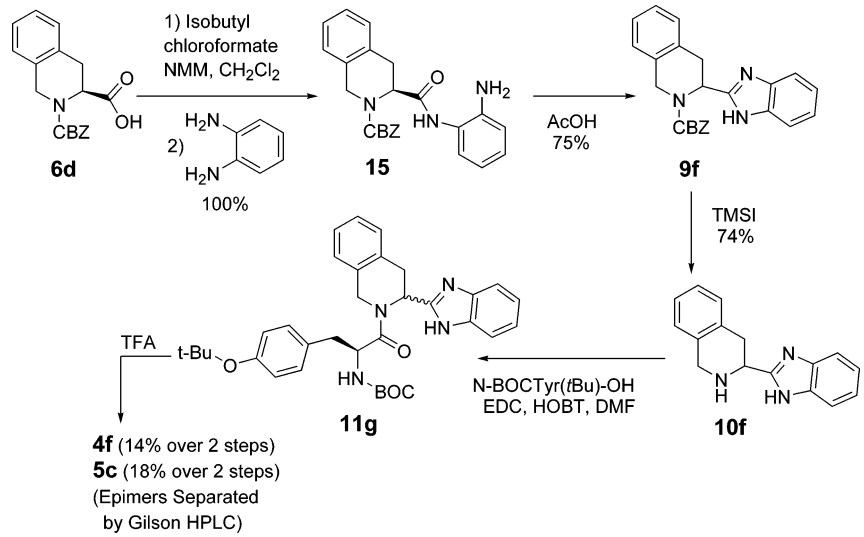

amide **11g** was carried on and deprotected to give approximately equal isolated quantities of products **4f** and **5c**. The respective products were characterized by comparing NMR data with related known imidazole diastereomers.

Results and Discussion

Our preliminary biological goal was to evaluate whether imidazoles **4** would be bioequivalent mimics of the amide opioid ligands **1**. We reasoned that this hypothesis would be validated if an imidazole **4** maintained consistent OR activity as its analogous amide **1**. Therefore as our initial gauge, we prepared imidazole **4a**, based on the knowledge that its directly related amide, **1b**, has been reported as a potent δ OR agonist.[5] We began our biological evaluation of **4a** by looking at its in vitro OR binding affinities for both the δ and μ receptors and were pleased to find that **4a** (K_i δ = 0.9 nM; K_i μ = 55 nM) maintained comparable binding affinities to that described for **1b** (K_i δ = 5.2 nM; K_i μ =

Table 2. δ and μ Opioid Receptors in Vitro Binding and Functional Activities

	binding data		selectivity	functional data	
no.	K_i δ[a] (nM)	K_i μ[a] (nM)	ratio (μ/δ)	EC_{50} δ[b] (nM)	EC_{50} μ[b] (nM)
1b	5.2[c]	69[c]	13[c]	82[d]	2120[d]
4a	0.9 ± 0.1	54.7 ± 12.5	63	25 (13)	2400 (2490)
4b	>100[e]	>100[e]	–	NT[f]	NT
4c	0.30 ± 0.04	20.7 ± 3.4	75	1.4 (3.5)	>10000[e]
4d	0.11 ± 0.04	11.6 ± 2.3	14	1.9 (5.8)	>10000[e]
4e	62.7 ± 20.4	>100[e]	>1	85 (43)	NT
4f	15.1 ± 0.7	>100[e]	>6	37(32)	>10000[e]
4h	21.5 ± 8.4	1.5 ± 0.8	0.1	542 (457)	153 (130)
4i	>100[e]	23.1 ± 2.4	<0.02	NT	1300
5a	19.4 ± 5.4	85.6 ± 10.1	4	127 (182)	NT
5b	>100[e]	>100[e]	–	NT	NT
5c	49.6 ± 27.7	>100[e]	>2	440 (261)	NT
Loperamide	50.1 ± 15.2	0.16 ± 0.1	0.003	156 (780)	58 (44)

[a] Average ($n = 3$) ± SE. [b] $n = 2$; i.e. Assay 1 (Assay 2). [c] Reported value;[5] values determined by displacement of selective radioligands from rat brain membrane preparations. [d] Reported value;[5] activities based on inhibition of electrically stimulated contractions of mouse vas deferens (MVD) for δ and of guinea pig ileum (GPI) for μ. [e] Tested twice. [f] NT = Not tested.

69 nM). Compound **4a** showed the least OR binding affinity at the κ OR (K_i κ = 124 nM). We subsequently evaluated **4a** for its δ OR functional activity via a GTPγS assay and were further encouraged to find that our parent imidazole **4a** behaved as a full δ OR agonist (EC_{50} δ = 13−25 nM). Compound **4a** possessed only modest μ OR functional agonist activity (EC_{50} μ = 2.4 μM via a GTPγS assay), which again was consistent with the profile reported for amide **1b**. Compound **4a** was also assessed for κ OR functional activity in a field stimulated rabbit vas deferens assay and was found to cause no inhibition of twitch contractions (EC_{50} > 30 μM). On the basis of **4a**'s preliminary in vitro results, which supported our hypothesis, we embarked on a cursory structure−activity-relationship (SAR) evaluation around our novel imidazoles **4**. These preliminary imidazoles are outlined in Table 1, and their corresponding in vitro OR results are compiled in Table 2; related experimental details for the in vitro assays are described in the Experimental Section.

To initiate our followup work around **4a**, we varied the 4,5-substituents of the imidazole as the first subset of analogues. We found that a simple addition of some lipophilicity at the R′ position of the imidazole, in place of the H of **4a**, slightly enhanced δ OR binding affinities. This conclusion is supported by comparing monovaried analogues **4c** and **4d** relative to **4a** [**4d** (R′ = Br; K_i δ = 0.11 ± 0.04 nM) > **4c** (R′ = Me; K_i δ = 0.3 ± 0.04 nM) > **4a** (R′ = H; K_i δ = 0.9 ± 0.1 nM)]. The δ OR functional SAR supported the same conclusion, using the δ OR GTPγS functional activities as the metric [**4c** (EC_{50} δ = 1.4−3.5 nM) ∼ **4d** (EC_{50} δ = 1.9−5.8 nM) > **4a** (EC_{50} δ = 13−25 nM)]. An additional comparison of trisubstituted imidazoles **4e** with **4a** clearly demonstrated that at the R″ position an aromatic moiety was preferable relative to an n-Pr aliphatic group for both δ and μ OR binding [**4e** (R″ = n-Pr; K_i δ = 63 nM; K_i μ >100 nM) ≪ **4c** (R″ = Ph; K_i δ = 0.3 nM; K_i μ = 21 nM)] and OR function [**4e** (EC_{50} δ = 43−85 nM) ≪ **4c** (EC_{50} δ 1.4−3.5 nM)]. We also prepared a trisubstituted fused phenyl imidazole, i.e., benzimidazole **4f**, whose activity could be directly compared to its respective nonfused trisubstituted phenyl imidazole analogue **4c**. We found that the 4-phenyl substituted imidazole **4c** proved significantly better in terms of δ (∼45-fold) and μ (>5-fold) OR binding affinities than the fused benzimidazole **4f** [**4c** (R′ = Me, R″ = Ph; K_i δ = 0.3 nM; K_i μ = 21 nM) > **4f** (R′, R″ = fused Ph; K_i δ = 15 nM; K_i μ > 100 nM)]. The associated δ OR GTPγS functional activities were reflective of the binding data, with the phenyl imidazole **4c** showing enhanced potency relative to benzimidazole **4f** [**4c** (EC_{50} δ = 1.4−3.5 nM) > **4f** (EC_{50} δ = 32−37 nM)].[14]

In addition to varying substitutions off the imidazole moiety of generic structure **4**, we also altered the isoquinoline core scaffold of **4c** to piperidine (**4h**) and pyrrolidine (**4i**). Both **4h** and **4i** had inverted δ to μ OR selectivity affinities relative to **4c**, with **4h** possessing considerable better OR affinities than **4i** [**4h** (piperidine; K_i δ = 21 nM; K_i μ = 2 nM); **4c** (isoquinoline; K_i δ = 0.3 nM; K_i μ = 21 nM); **4i** (pyrrolidine; K_i δ >100 nM; K_i μ = 23 nM)]. Although the relative binding affinities for piperidine **4h** compared to pyrrolidine **4i** were rather informative, the inverted μ/δ selectivity ratio for both nonfused heterocycles **4h** and **4i** relative to isoquinoline **4c** was less enlightening, as it's consistent with previous reports for similar scaffold variations in amide-associated opioids.[15] Consistent with the previous OR binding to function activity comparisons, the related functional activities for this subset of compounds were reflective of their binding affinities [**4h** (EC_{50} δ = 542 nM) < **4c** (EC_{50} δ 1.4−3.5 nM); **4h** (EC_{50} μ = 130−153 nM) > **4i** (EC_{50} μ = 1300 nM) > **4c** (EC_{50} δ >10 μM)].

The last subset of compounds evaluated for in vitro activity was comprised of **5a**, **5b**, and **5c**, the respective epimers of **4c**, **4e**, and **4f**. In all comparable cases, the *S,S* configuration was the preferred stereochemistry for optimized δ OR affinity binding [**4c** (*S,S*; K_i δ = 0.3 nM; K_i μ = 21 nM) > **5a** (*R,S*; K_i δ = 19 nM; K_i μ = 86 nM); **4e** (*S,S*; K_i δ = 63nM; K_i μ >100 nM) > **5b** (*R,S*; K_i δ >100 nM; K_i μ >100 nM); **4f** (*S,S*; K_i δ = 15 nM; K_i μ >100 nM) > **5c** (*R,S*; K_i δ = 50 nM; K_i μ > 100 nM)], as well as for optimized OR functional activity [**4c** (EC_{50} δ 1.4−3.5 nM) > **5a** (EC_{50} δ 127−182 nM); **4f** (EC_{50} δ 32−37 nM) > **5c** (EC_{50} δ 261−440 nM)].

We also tested our previously reported potent TPPII imidazole inhibitor **4b** for OR in vitro activity. Not surprisingly, **4b** was found void of any significant OR affinity (K_i δ >100 nM; K_i μ >100 nM).

Having found that compound **4a** was a potent OR ligand, we were curious how it would overlay in silico relative to a previously reported peptidyl compound

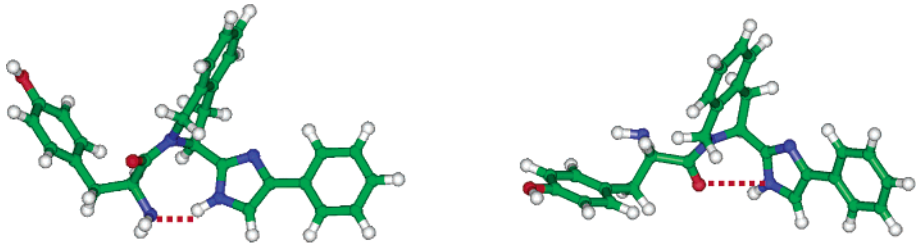

Figure 2. Two lowest energy conformers of compound **4a**. The intramolecular hydrogen bonds are shown in red dash lines.

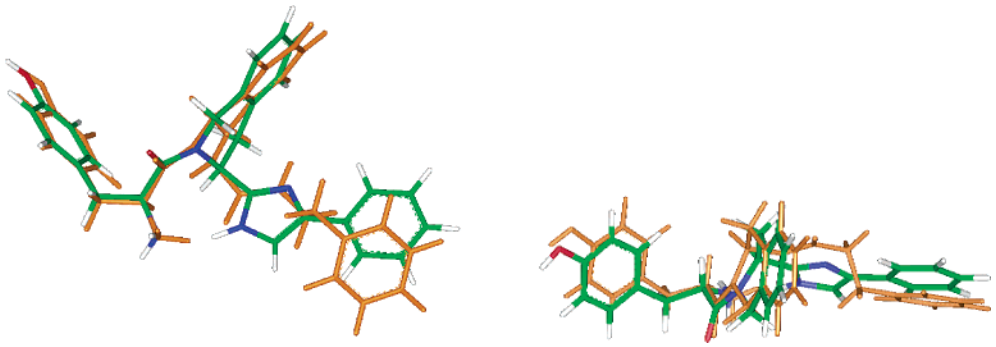

Figure 3. Complimentary orthogonal views for superimposition of compound **4a** over **1b** (in orange).

such as **1b**. To initiate this modeling work, we did a conformational search and energy minimization of imidazole **4a**, using the methodology and software described in the Experimental Section. This initial modeling exercise yielded conformers I and II among the lowest energy conformers (Figure 2). Conformer-I contains an intramolecular hydrogen bond between the NH_2 amine nitrogen and the imidazole NH hydrogen, while Conformer-II possesses an intramolecular hydrogen bond between the NH hydrogen of the imidazole and the oxygen of the carbonyl group. A computation of relative energies between these two conformers revealed that Conformer-I is about 0.5 kcal/mol more stable than Conformer-II, based on Merck Molecular Force Field (MMFF)[16] calculations. To further validate that Conformer-I was preferred over Conformer-II, high-level quantum chemical calculations were carried out on the two conformers. This additional study confirmed Conformer-I as the preferred conformer by 2.7 kcal/mol relative to Conformer-II. Having identified Conformer-I as an energy-minimized structure of **4a**, we then generated a lowest energy conformation of modified dipeptide **1b**. We were encouraged to see that our energy-minimized structure for **1b** was very similar to a previously calculated conformation[17] for related analogue H-Dmt-Tic-NH−CH_2−BID, whose conformation was based on a recent X-ray crystal structure of N,N-$(Me)_2$-DMT-Tic-OH.[18] To complete our modeling exercise, we overlaid the energy-minimized structures **4a** and **1a**, which readily demonstrates the favorable overlap of all key pharmacophore elements for the two structures (Figure 3). Although the in vitro and in silico results for compounds **4** proved quite favorable, the key and foremost question remained, i.e. how would imidazoles **4** behave in vivo.

It is well-known that opioids can induce in vivo effects centrally and/or peripherally, eliciting analgesic and/or GI responses. To measure **4**'s potential in vivo effects, we focused on a preliminary set of classical in vivo analgesic and GI assays to ascertain an initial profile for this new series. The mouse abdominal irritant test (MAIT) was utilized to assess central analgesic activity, while the mouse glass bead expulsion test (MGBET) and the mouse fecal pellet output test (MFPOT) were employed to appraise GI propulsive motility effects. Compound **4a** was chosen as a representative compound for the preliminary in vivo profiling. It was predetermined that to fairly judge **4a** as a practical medicinal chemistry lead, related in vivo activities would have to be observed from systemic administration. Although peptidyl-like compounds are often reported in the literature as extremely potent in vivo when administration is intracerebroventricular (icv), we felt this route of administration should be utilized simply as a proof of principle (POP) exercise.

Compound **4a** possessed no activity (0% inhibition of abdominal constriction) in the MAIT at a dose of 100 mg/kg when dosed subcutaneously (sc). As a POP followup, compound **4a** was dosed icv in the MAIT and was found to exhibit a 40% inhibition of abdominal constriction at a dose of 10 μg, and a 100% inhibition at a dose of 100 μg. These results suggest that **4a** does possess OR-mediated analgesic activity, but that **4a** does not cross the blood−brain barrier. With regard to the in vivo GI screens, compound **4a** inhibited reflex-stimulated colonic propulsion in a dose-dependent manner in the MGBET when dosed intraperitoneal (ip) at 3, 5, and 10 mg/kg (Figure 4). Subsequently we showed that **4a**'s inhibition of colonic propulsion in the MGBET was blocked by the OR antagonist naloxone (ip), which is supportive evidence that **4a**'s MGBET in vivo effects are OR mediated (Figure 5). Compound **4a**'s GI effectiveness was also corroborated with the MFPOT, where it was found that **4a** significantly attenuated fecal pellet output at 1 and 3 mg/kg for at least 6 h following ip administration (Figure 6).

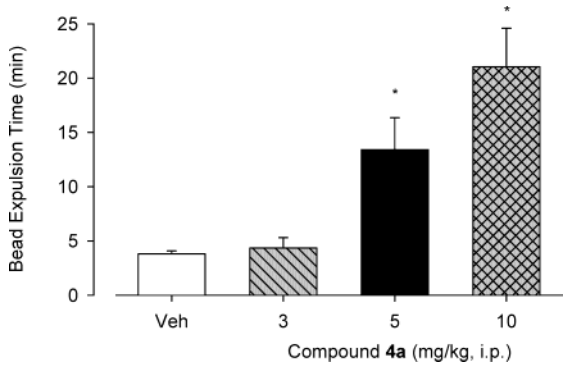

Figure 4. Compound **4a** (JNJ-10335572) inhibits reflex-stimulated colonic propulsion in a dose-dependent manner. * $P < 0.05$ vs vehicle.

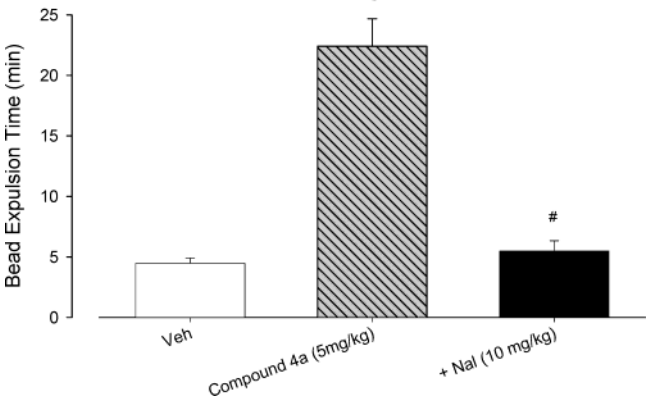

Figure 5. Compound **4a** (JNJ-10335572) inhibits reflex-stimulated colonic propulsion in a naloxone-sensitive manner. * $P < 0.05$ vs vehicle; # $P < 0.05$ vs compound **4a**.

These in vivo results demonstrate that **4a** possesses OR activities, and that these effects are restricted to the periphery. Consequently, these results suggest that closely related compounds of **4a** might prove useful for GI indications. As a result, most followup synthetic efforts have been steered in that direction.

In conclusion, we have identified novel imidazoles **4** as extremely potent δ OR agonists, and their in vitro OR activities are reflective of the activities reported for amides **1**. These related in vitro results correlate well with our molecular modeling work, where we showed that an energy-minimized structure of imidazole **4a** overlays nicely with an energy-minimized conformer of amide **1b**. Our preliminary in vivo evaluation of a representative imidazole, **4a**, revealed that its OR activity is limited to peripheral modes of action when administered systemically, i.e., **4a** affected GI motility while demonstrating no apparent central analgesic affects. Further chemical and biological endeavors around these opioid efforts are currently underway.

Experimental Section

Novel compounds listed in Table 1, i.e. final products **4a**, **4c**−**f**, **4h**, **4i**, and **5a**−**c**, were all characterized by 300-MHz ^{1}H NMR (Bruker-Biospin, Inc. DPX-300), mass spectra (Finnegan 3300), and HPLC (>99% purity at 214 nm and 254 nm; Hewlett-Packard Series 1050 HPLC with a 3 μm, 3.3 mm × 50 mm Supelco AZB+ C18 column using a gradient mobile phase of 4:96:0.1 acetonitrile/water/TFA to 100:0:0.1 acetonitrile/water/TFA over 8.5 min, at a flow rate of 1.20 mL/min and a total run time of 9.5 min). These final products were also assayed for homogeneity by TLC on Whatman MK6F (1 in. x 3 in. × 250 um) silica gel plates. These final products were also evaluated by high-resolution mass spectrum (HRMS) analyses (Autospec E high resolution magnetic sector mass spectrometer). The HRMS analyses were carried out internally by our Spectroscopy Department in Spring House, PA. Representative final product **4a** was also analyzed by combustion analyses for C, H, and N, which were carried out by Robertson Microlit Laboratories, Inc, Madison, NJ. The results from this analysis suggest that the final products are diaddition TFA salts, and related biological data are reflected as such. The related ^{1}H NMR spectra data for all final products, as well as representative intermediates, are included in the Experimental Section. Intermediates were also assayed by HPLC, HPLC/MS, and/or TLC, with related data also included in the Experimental Section. All reagents were commercially available unless otherwise specified, and all reactions were run under an inert atmosphere of Ar or N_2. Where required, preparative purifications were performed on a Gilson semi-preparative HPLC unit (Column: YMC ODS-A 30 × 100 mm, 5 μm; temperature: ambient; flow rate: 35 mL/min; mobile phase: (A) 10/90 acetonitrile/ water with 0.1% trifluoroacetic acid, (B) 90/10 acetonitrile/ water with 0.1% trifluoroacetic acid; gradient: linear gradient from A to B over 9 min; wavelength: 214 and 254 nm).

Molecular Modeling. Conformational searching for **1b** and **4a** were carried out by molecular dynamics (MD) simulations using Sybyl 6.8 software[19] of Tripos. Merck Molecular Force Field (MMFF)[16] and charges were used for molecular dynamic (MD) simulations and the following energy minimizations. The MD simulations were run for 500 ps in a vacuum with a dielectric constant $\epsilon = 1$ at 700 K in order to sample various conformations for the six member aliphatic rings in all these three molecules. Conformations were saved at each 1 ps along the MD trajectories and then were energy minimized using conjugated gradient method for 1000 iterations. Conformer-I and −II were optimized using density functional method at

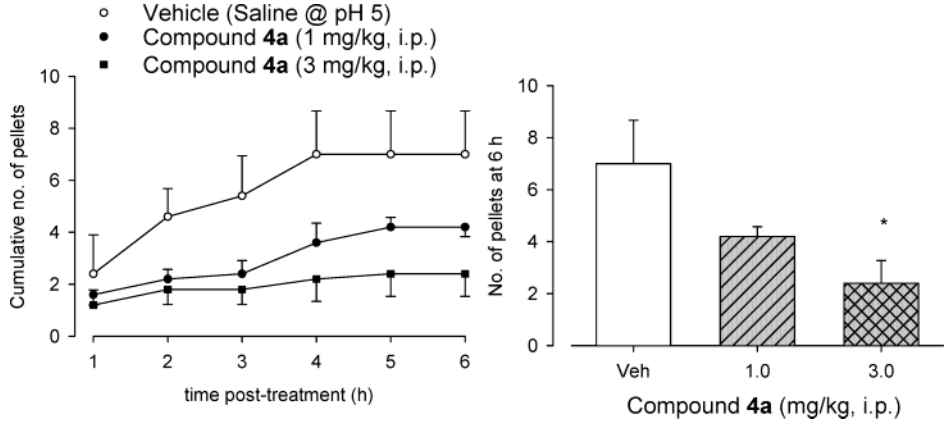

Figure 6. Compound **4a** (JNJ-10335572) reduces fecal pellet output in a dose-dependent manner. * $P < 0.05$ vs vehicle.

B3LYP/6-31G** level in the quantum chemistry package Jaguar 5.5., Schrodinger L.L.C.(1500 SW First Ave, Portland, OR 97201).

Syntheses. (*S*)-3-(2-Oxo-2-phenyl-ethylcarbamoyl)-3,4-dihydro-1*H*-isoquinoline-2-carboxylic Acid *tert*-Butyl Ester (8a). Compounds **6a** (Aldrich) (2.77 g, 10 mmol), **7a** (Aldrich) (1.71 g, 10 mmol), and HOBT (2.70 g, 20 mmol) were dissolved in dichloromethane (CH_2Cl_2) (100 mL). The solution was cooled to 0 °C and then EDC (2.29 g, 12 mmol) was added followed by *N*-methyl-morpholine (NMM) (1.31 g, 13 mmol). The reaction mixture was then warmed to room temperature (RT). After 72 h the mixture was extracted with water, and the organic phase was extracted consecutively with aqueous solutions of saturated $NaHCO_3$, 2 N citric acid, and saturated $NaHCO_3$ once again. The organic phase was then dried over $MgSO_4$, filtered, and concentrated to yield 3.95 g (T.W. 3.94 g) of **8a** as a yellow foam, which was used without further purification (HPLC: 86% at 214 nm; HPLC/MS: *m*/*z* 395 (MH^+); TLC: 80:20:5 $CHCl_3$:CH_3OH:HCOOH, R_f = 0.82) ^{1}H NMR ($CDCl_3$) δ 1.4−1.65 (d, 9H), 3.0−3.2 (m, 1H), 3.2−3.45 (m, 1H), 4.45−4.8 (m, 4H), 6.8−7.0 (s, 0.5H), 7.05−7.3 (m, 3.5H), 7.4−7.5 (t, 2H), 7.6−7.7 (t, 1H), 8.9−8.95 (d, 2H).

(2S)-2-[(1*RS*)-1-Methyl-2-oxo-2-phenyl-ethylcarbamoyl]-piperidine-1-carboxylic Acid Benzyl Ester (8b). Starting from **6b** (Aldrich) and **7b**,[20] compound **8b** was prepared in a similar manner as **8a** and was used for its subsequent reaction without further purification (crude yield: ∼100%; HPLC: 99% at 214 nm; HPLC/MS: *m*/*z* 395 (MH^+)).

(2*S*)-2-[(1*RS*)-1-Methyl-2-oxo-2-phenyl-ethylcarbamoyl)-pyrrolidine-1-carboxylic Acid Benzyl Ester (8c). Starting from **6c** (Aldrich) and **7b**,[20] compound **8c** was prepared in a similar manner as **8a** and was used for its subsequent reaction without further purification (crude yield: ∼100%; HPLC: 92% at 214 nm; HPLC/MS: *m*/*z* 381 (MH^+)).

(*S*)-3-(4-Phenyl-1*H*-imidazol-2-yl)-3,4,-dihydro-1*H*-isoquinoline-2-carboxylic Acid *tert*-Butyl Ester (9a). Intermediate **8a** (3.55 g, 9 mmol), NH_4OAc (20.8 g, 270 mmol), and AcOH (30 mL) were combined at RT, and the reaction mixture was warmed on a steam bath for about 3 h. The reaction mixture was then cooled to RT and poured into an ice slurry mix (400 g). To this mixture were added concentrated ammonium hydroxide (NH_4OH; 50 mL) and ethyl ether (Et_2O). The layers were separated, and the aqueous phase washed with a second portion of Et_2O. The organic phases were combined, dried over $MgSO_4$, filtered, and concentrated under reduced pressure to yield 3.51 g of brown foam. This crude sample was purified by preparative HPLC to yield 0.85 g (25%) of **9a** as a white lyophile (HPLC: 96% at 214 nm; HPLC/MS: *m*/*z* 376 (MH^+); TLC: 80:20:5 $CHCl_3$:CH_3OH:HCOOH, R_f = 0.77) ^{1}H NMR ($CDCl_3$) δ 1.2 (br s, 3H), 1.45 (br s, 6H), 3.1−3.45 (br m, 2H), 4.45−4.7 (br m, 2H), 5.3−5.7 (br m, 1H), 6.9−7.6 (bm, 9H).

(*S*)-2-(4-Methyl-5-phenyl-1*H*-imidazol-2-yl)-piperidine-1-carboxylic Acid Benzyl Ester (9b). Intermediate **8b** (0.59 g, 1.5 mmol) was dissolved in RT xylenes (20 mL), then NH_4-OAc (2.89 g, 37.5 mmol) and AcOH (1 mL) were added. This mixture was placed in an oil bath and warmed to 160 °C with water being azeotroped into a Dean−Stark trap. After 2 h the mixture was cooled to RT and extracted with brine. The resulting organic phase was dried over $MgSO_4$, filtered, and concentrated under reduced pressure to give 0.61 g (T.W. 0.56 g) of **9b** as a brown oil, which was used without further purification (HPLC: 98% at 254 nm; HPLC/MS: *m*/*z* 376 (MH^+)).

(*S*)-2-(4-Methyl-5-phenyl-1*H*-imidazol-2-yl)-pyrrolidine-1-carboxylic Acid Benzyl Ester (9c). Starting from **8c**, compound **9c** was prepared in a similar manner as **9b** and was used for its subsequent reaction without further purification (crude yield: ∼100% of brown oil; HPLC: 98% at 254 nm; HPLC/MS: *m*/*z* 362 (MH^+); TLC: 80:20:5 $CHCl_3$:CH_3OH:HCOOH, R_f = 0.55, homogeneous).

(*S*)-3-(5-Methyl-4-phenyl-1*H*-imidazol-2-yl)-3,4-dihydro-1*H*-isoquinoline-2-carboxylic Acid *tert*-Butyl Ester (9d). 3-Formyl-3,4-dihydro-1*H*-isoquinoline-2-carboxylic acid *tert*-butyl ester (**12**)[12] (1.83 g, 7 mmol) was combined with AcOH (25 mL). To this mixture were immediately added **13a** (Aldrich) (3.11 g, 21 mmol) and NH_4OAc (13.49 g, 175 mmol). The reaction mixture was then placed on a steam bath and heated for 20 min. The reaction mixture was cooled in an ice bath and then added to an ice slurry (400 g). The resulting mixture was basified by addition of concentrated NH_4OH (50 mL) and then extracted twice with Et_2O (150 mL each). The combined organic phases were dried over $MgSO_4$, filtered and concentrated to yield 5.25 g of crude product. This material was purified by preparative HPLC to yield 1.40 g (51%) of **9d** as a white lyophil.(TLC:80:20:5 $CHCl_3$:CH_3OH:HCOOH, R_f = 0.65).

(*S*)-3-(5-Methyl-4-propyl-1H-imidazol-2-yl)-3,4-dihydro-1*H*-isoquinoline-2-carboxylic Acid *tert*-Butyl Ester (9e). Starting from **13b** (Aldrich), **9e** was prepared in a similar manner as **9d** (Yield: 54%; HPLC: 98% at 214 nm).

3-(1*H*-Benzoimidazol-2-yl)-3,4-dihydro-1*H*-isoquinoline-2-carboxylic Acid Benzyl Ester (9f). Intermediate **15** (2.0 g, 5 mmol) was added to AcOH (70 mL) and warmed to reflux for 1.5 h. The solvent was then removed under reduced pressure and the residue partitioned between Et_2O and saturated aqueous $NaHCO_3$. The organic phase was dried over $MgSO_4$, filtered, and concentrated under reduced pressure to give 1.44 g (75%) of **9f** as an off white solid, which was used without further purification (HPLC: 91% at 254 nm; HPLC/MS: *m*/*z* 384 (MH^+); TLC: 80:20:5 $CHCl_3$:CH_3OH:HCOOH, R_f = 0.73). Noteworthy is that compound **9f** gave two distinct peaks of similar intensity on three separate chiral columns − Daicel Chiralcel OD-H, Daicel Chiralcel AD-H, and Daicel Chiralcel OJ-H. Each column run utilized the same conditions: 95/5 to 60/40 hexane/IPA with an equilibrium time of 13 min, an initial hold time of 5 min, a gradient of 1.75%/min, a gradient time of 20 min and a final hold time of 5 min. In addition, the data from column Daicel Chiralcel AD-H included a distinct polarimeter trace indicating the separated peaks had opposite polarities. Conversely, starting material **15** showed no separation on the chiral columns.

(*S*)-3-(4-Phenyl-1*H*-imidazol-2-yl)-1,2,3,4-tetrahydro-isoquinoline (**10a**). Intermediate **9a** (0.75 g, 2 mmol) was added to 0 °C neat TFA (4 mL). The reaction mixture was allowed to warm to room temperature over about 45 min. Excess TFA was removed under a stream of N_2. The residue was partitioned between CH_2Cl_2 (15 mL) and saturated aqueous $NaHCO_3$. The aqueous phase was then re-extracted with a second portion of CH_2Cl_2, and the organic phases were combined, dried over $MgSO_4$, and filtered, to yield **10a** as a solution in CH_2Cl_2. This solution was used in the next step without further purification or isolation. A small portion was concentrated under reduced pressure for NMR purposes. (HPLC: 99% at 214 nm; HPLC/MS: *m*/*z* 276 (MH^+); TLC: 80:20:5 $CHCl_3$:CH_3OH:HCOOH, R_f= 0.36, homogeneous) ^{1}H NMR (DMSO-d_6) δ 3.15−3.25 (d, 2H), 4.1−4.25 (dd, 2H), 4.3−4.4 (t, 1H), 7.1−7.25 (t, 4H), 7.3−7.4 (t, 3H), 7.55−7.6 (s, 1H), 7.75−7.8 (d, 2H)).

(*S*)-2-(4-Methyl-5-phenyl-1*H*-imidazol-2-yl)-piperidine (10b). Intermediate **9b** (0.56 g, 1.5 mmol) was dissolved in $CHCl_3$ (20 mL) at 20 °C, and then TMSI (0.64 mL, 4.5 mmol) was added neat. After 16 h the reaction was concentrated under reduced pressure and the residue was treated with CH_3-OH (7 mL) followed by 2 N HCl (aq) (2 mL). The resulting mixture was warmed on a steam bath for 3 h. The mixture was then concentrated to remove the majority of CH_3OH, and to the resulting mixture was added 1 N HCl (aq) (6 mL). This aqueous mixture was extracted twice with Et_2O and then cooled and basified with 3 N NaOH (aq). The basic solution was extracted thrice with $CHCl_3$ (15 mL each). The combined $CHCl_3$ layers were dried over $NaSO_4$, filtered, and concentrated under reduced pressure to give 284 mg (79%) of **10b**, which was used without further purification (HPLC: 99% at 214 nm; HPLC/MS: *m*/*z* 242 (MH^+); 80:20:5 $CHCl_3$:CH_3OH: HCOOH, R_f = 0.27, homogeneous).

(*S*)-4-Methyl-5-phenyl-2-pyrrolidin-2-yl-1*H*-imidazole (10c). Starting from **9c**, **10c** was prepared in a similar manner as **10b** (Yield: 77%; HPLC: 100% at 214 nm; HPLC/

MS: *m*/*z* 228 (MH^+); TLC: 80:20:5 $CHCl_3$:CH_3OH:HCOOH, $R_f = 0.13$, homogeneous).

(*S*)-3-(5-Methyl-4-phenyl-1*H*-imidazol-2-yl)-1,2,3,4-tetrahydro-isoquinoline (10d). Starting from **9d**, **10d** was prepared in a similar manner as **10a**. As with **10a**, the CH_2Cl_2 solution of **10d** was used directly without further manipulation.

(*S*)-3-(4-Methyl-5-propyl-1*H*-imidazol-2-yl)-1,2,3,4-tetrahydro-isoquinoline (10e). Starting from **9e**, **10e** was prepared in a similar manner as **10a**. As with **10a**, the CH_2Cl_2 solution of **10e** was used directly without further manipulation (TLC: 80:20:5 $CHCl_3$:CH_3OH:HCOOH, $R_f = 0.4$, homogeneous).

3-(1*H*-Benzoimidazol-2-yl)-1,2,3,4-tetrahydro-isoquinoline (10f). Starting from **9f**, **10f** was prepared in a similar manner as **10b** (Yield: 74%; HPLC: 93% at 214 nm; HPLC/MS: *m*/*z* 250 (MH^+); 80:20:5 $CHCl_3$:CH_3OH:HCOOH, $R_f = 0.30$, homogeneous).

[(1*S*)-1-(4-*tert*-Butoxy-benzyl)-2-oxo-2-[(3*S*)-3-(4-phenyl-1*H*-imidazol-2-yl)-3,4-dihydro-1*H*-isoquinolin-2-yl]-ethyl]-carbamic Acid *tert*-Butyl Ester (11a). 2-*tert*-Butoxycarbonylamino-3-(4-*tert*-butoxy-phenyl)-propionic acid (BOC-Tyr(*t*Bu)-OH; Advanced ChemTech) (0.74 g, 2.2 mmol) was dissolved in CH_2Cl_2 (40 mL) and the reaction mixture cooled to about 0 °C. To the solution was added NMM (0.21 g, 2.1 mmol) followed by isobutyl chloroformate (0.27 g, 2 mmol, 0.26 mL), and the solution was allowed to stand for about 1.25 h. To the reaction mixture was then added the solution of **10a** (0.55 g, 2 mmol) and the reaction mixture stirred for about 16 h. The reaction mixture was then extracted with water, saturated aqueous $NaHCO_3$, 2 N citric acid, and saturated aqueous $NaHCO_3$ again, dried over $MgSO_4$, filtered, and concentrated to yield 1.10 g (93%) of **11a** as a foam, which was used without further purification (HPLC: 67% pure (5.30 min) at 254 nm; HPLC/MS: *m*/*z* 595 (MH^+); TLC: 80:20:5 $CHCl_3$:CH_3OH:HCOOH, $R_f = 0.87$, homogeneous).

{(1*S*)-1-(4-*tert*-Butoxy-benzyl)-2-[(2*S*)-2-(4-methyl-5-phenyl-1*H*-imidazol-2-yl)-piperidin-1-yl]-2-oxo-ethyl}-carbamic Acid *tert*-Butyl Ester (11b). Starting from **10b**, **11b** was prepared in a similar manner as **11a** (Yield: 97%; HPLC: 71% pure (5.15 min) at 254 nm; HPLC/MS: *m*/*z* 561 (MH^+); TLC: 80:20:5 $CHCl_3$:CH_3OH:HCOOH, $R_f = 0.77$, homogeneous).

{(1*S*)-1-(4-*tert*-Butoxy-benzyl)-2-[(2*S*)-2-(4-methyl-5-phenyl-1*H*-imidazol-2-yl)-pyrrolidin-1-yl]-2-oxo-ethyl}-carbamic Acid *tert*-Butyl Ester (11c). Starting from **10c**, **11c** was prepared in a similar manner as **11a** (Yield: 82%; HPLC: 92% pure (4.98 min) at 254 nm; HPLC/MS: *m*/*z* 547 (MH^+); TLC: 80:20:5 $CHCl_3$:CH_3OH:HCOOH, $R_f = 0.64$, homogeneous).

[2-[(3*S*)-3-(4-Bromo-5-phenyl-1*H*-imidazol-2-yl)-3,4-dihydro-1*H*-isoquinolin-2-yl]-(1*S*)-1-(4-*tert*-butoxy-benzyl)-2-oxo-ethyl]-carbamic Acid *tert*-Butyl Ester (11d). To a 0 °C solution of **11a** (0.18 g, 0.3 mmol) in $CHCl_3$ (5 mL) was added a solution of Br_2 (0.015 mL, 0.3 mmol) in $CHCl_3$ (1 mL) over 1 min. After 1h at 0 °C the mixture was extracted with cold saturated aqueous $NaHCO_3$. The organic phase was dried over $MgSO_4$, filtered, and concentrated under reduced pressure to give 220 mg (T.W. 202 mg) of **11d** as a brown foam, which was used without further purification (HPLC: 79% pure (7.22 min.) at 254 nm; HPLC/MS: *m*/*z* 673 (MH^+)).

{(1*S*)-1-(4-*tert*-Butoxy-benzyl)-2-[(3*S*)-3-(4-methyl-5-phenyl-1*H*-imidazol-2-yl)-3,4-dihydro-1*H*-isoquinolin-2-yl]-2-oxo-ethyl}-carbamic Acid *tert*-Butyl Ester (11e). Starting from **10d**, **11e** was prepared in a similar manner as **11a**. The final crude product isolated (1.55 g; 90%) proved to be an isomeric mixture of epimers, based on HPLC and HPLC/MS analysis. By HPLC, there proved to be 49% (5.47 min) of desired **11e** in the crude reaction mixture and 23% (5.60 min) of its related epimer **14a**. These compounds were separated by preparative HPLC purification yielding 310 mg (18%) of desired **11e** and 50 mg (3%) of **14a**. (**11e**: HPLC/MS: *m*/*z* 609 (MH^+); TLC: 80:20:5 $CHCl_3$:CH_3OH:HCOOH, $R_f = 0.79$, homogeneous).

{(1*S*)-1-(4-*tert*-Butoxy-benzyl)-2-[(3*S*)-3-(4-methyl-5-propyl-1*H*-imidazol-2-yl)-3,4-dihydro-1*H*-isoquinolin-2-yl]-2-oxo-ethyl}-carbamic Acid *tert*-Butyl Ester (11f). Starting from **10e**, **11f** was prepared in a similar manner as **11a.** The final crude product isolated (270 mg; T.W. 242 mg) proved to be an isomeric mixture of epimers, based on HPLC and HPLC/MS analysis. By HPLC, there proved to be 48% (5.33 min) of desired **11f** in the crude reaction mixture, and 33% (5.48 min) of its related epimer **14b**. These compounds were separated by preparative HPLC purification yielding 100 mg (41%) of desired **11f** and 10 mg (4%) of **14b**. (**11f**: HPLC/MS: *m*/*z* 574 (MH^+); TLC: 80:20:5 $CHCl_3$:CH_3OH:HCOOH, $R_f = 0.75$, homogeneous).

[2-[3-(1*H*-Benzoimidazol-2-yl)-3,4-dihydro-1*H*-isoquinolin-2-yl]-1-(4-*tert*-butoxy-benzyl)-2-oxo-ethyl]-carbamic Acid *tert*-Butyl Ester (11g). Intermediate **10f** (0.160 g, 0.6 mmol), BOC-Tyr(*t*Bu)-OH (0.22 g, 0.6 mmol), and HOBT (2.70 g, 1.28 mmol) were dissolved in DMF, and then EDC (0.15 g, 0.77 mmol) was added at RT. After 16 h the mixture was partitioned between water and EtOAc. The organic phase was re-extracted with water, dried over $MgSO_4$, filtered, and concentrated to yield 0.39 g (T.W. 0.34 g) of **11g** as an orange foam, which was used without further purification.

{(1*S*)-1-(4-*tert*-Butoxy-benzyl)-2-[(3*R*)-3-(4-methyl-5-phenyl-1*H*-imidazol-2-yl)-3,4-dihydro-1*H*-isoquinolin-2-yl]-2-oxo-ethyl}-carbamic Acid *tert*-Butyl Ester (14a). The isolation of this product is described under conditions for **11e**. (**14a**: HPLC/MS: *m*/*z* 574 (MH^+); TLC: 80:20:5 $CHCl_3$:CH_3OH:HCOOH, $R_f = 0.68$).

{(1*S*)-1-(4-*tert*-Butoxy-benzyl)-2-[(3*R*)-3-(4-methyl-5-propyl-1*H*-imidazol-2-yl)-3,4-dihydro-1*H*-isoquinolin-2-yl]-2-oxo-ethyl}-carbamic Acid *tert*-Butyl Ester (14b). The isolation of this product is described under conditions for **11f**. (**14b**: HPLC/MS: *m*/*z* 574 (MH^+); TLC: 80:20:5 $CHCl_3$:CH_3OH:HCOOH, $R_f = 0.65$).

(*S*)-3-(2-Amino-phenylcarbamoyl)-3,4-dihydro-1*H*-isoquinoline-2-carboxylic Acid Benzyl Ester (15). Starting material **6d** (1.56 g, 5 mmol) was dissolved in CH_2Cl_2 (40 mL) and the reaction mixture cooled to about 0 °C. To the solution was added NMM (0.51 g, 5 mmol) followed by isobutyl chloroformate (0.68 g, 2 mmol), and the solution was allowed to stand for 1 h. 1,2-Phenylenediamine (0.54 g, 5 mmol) in CH_2Cl_2 (10 mL) was then added and the reaction mixture stirred for 3 h. The reaction mixture was then extracted with water, dried over $MgSO_4$, filtered, and concentrated to yield 2.11 g (T.W.2.01 g) of **15** as an off white solid, which was used without further purification (HPLC: 100% at 214 nm; TLC: 80:20:5 $CHCl_3$:CH_3OH:HCOOH, $R_f = 0.73$, homogeneous).

(2*S*)-2-Amino-3-(4-hydroxy-phenyl)-1-[(3*S*)-3-(5-phenyl-1*H*-imidazol-2-yl)-3,4-dihydro-1*H*-isoquinolin-2-yl]-propan-1-one Trifluoroacetate Hydrate (1:2:1) (4a). TFA (4 mL) was cooled to about 0 °C, and then **11a** (1.10 g, 1.85 mmol) was added. The reaction mixture sat for about 0.5 h. Excess TFA was then removed under a stream of N_2 to yield a brown oil. The oil was purified via preparative HPLC to yield 600 mg of **4a** as a white lyophile (HPLC: 100% at 214 and 254 nm; HPLC/MS: *m*/*z* 439 (MH^+); TLC: 80:20:5 $CHCl_3$:CH_3OH:HCOOH, $R_f = 0.32$, homogeneous). ^1H NMR (MeOH-d_4) δ 2.1−2.25 (dd, 0.3H), 3.0−3.6 (m, 3.7H), 4.6−4.85 (m, 3H), 5.2−5.35 (t, 0.3H), 5.6−5.7 (t, 0.7H), 6.7−6.75 (d, 1.4H), 6.8−6.85 (d, 0.6H), 7.05−7.1 (d, 1.4H), 7.15−7.2 (d, 1.6H), 7.35−7.65 (m, 6H), 7.75−7.8 (d, 2H), 7.85 (s, 1H). HRMS calcd for $C_{27}H_{26}N_4O_2$ (MH^+): 439.2134. Found: 439.2146. Anal. ($C_{27}H_{26}N_4O_2/2C_2HF_3O_2/H_2O$): Calc'd: C: 54.39; H: 4.42; N: 8.18, Found: C: 54.13; H: 4.45; N: 7.91.

(2*S*)-2-Amino-3-(4-hydroxy-phenyl)-1-[(3*S*)-3-(4-methyl-5-phenyl-1*H*-imidazol-2-yl)-3,4-dihydro-1*H*-isoquinolin-2-yl]-propan-1-one Trifluoroacetate (1:2) (4c). Starting from **11e**, **4c** was prepared in a similar manner as **4a** (Yield: 71%; HPLC: 100% at 214 and 254 nm; HPLC/MS: *m*/*z* 453 (MH^+); TLC: 80:20:5 $CHCl_3$:CH_3OH:HCOOH, $R_f = 0.37$, homogeneous). ^1H NMR (MeOH-d_4) δ 2.25 (s, 1H), 2.45 (s, 2H), 3.0−3.6 (m, 4H), 4.4−4.6 (m, 1H), 4.7−5.0 (m, 2H), 5.15−5.25 (m, 0.3H), 5.65−5.75 (t, 0.7H), 6.7−6.75 (m, 2H), 7.0−7.2 (m,

3.5H), 7.25−7.35 (m, 4H), 7.5−7.65 (m, 3.5H). HRMS calcd for $C_{28}H_{28}N_4O_2$ (MH^+): 453.2290. Found: 453.2291.

(2*S*)-2-Amino-1-[(3*S*)-3-(4-bromo-5-phenyl-1*H*-imidazol-2-yl)-3,4-dihydro-1*H*-isoquinolin-2-yl]-3-(4-hydroxy-phenyl)-propan-1-one Trifluoroacetate (1:2) (4d). Starting from **11d**, **4d** was prepared in a similar manner as **4a** (Yield: 23%; HPLC: 99.3% at 214 and 100% at 254 nm; HPLC/MS: *m*/*z* 517 (MH^+); TLC: 80:20:5 $CHCl_3$:CH_3OH:HCOOH, R_f = 0.55, homogeneous). ^{1}H NMR (MeOH-d_4) δ 2.0−2.1 (dd, 0.6H), 2.9−3.4 (m, 3.4H), 4.2−4.3 (d, 0.6H), 4.45−4.6 (m, 1H), 4.65−4.95 (m, 3.2H), 5.45−5.5 (t, 0.4H), 6.5−6.55 (d, 2H), 6.9−7.1 (m, 4H), 7.15−7.4 (m, 5.4H), 7.6−7.65 (d, 0.6H). HRMS calcd for $C_{27}H_{25}BrN_4O_2$ (MH^+): 517.1239. Found: 517.1257.

(2*S*)-2-Amino-3-(4-hydroxy-phenyl)-1-[(3*S*)-3-(4-methyl-5-propyl-1*H*-imidazol-2-yl)-3,4-dihydro-1*H*-isoquinolin-2-yl]-propan-1-one Trifluoroacetate (1:2) (4e). Starting from **11f**, **4e** was prepared in a similar manner as **4a** (Yield: 17%; HPLC: 99.3% at 214 and 100% at 254 nm; HPLC/MS: *m*/*z* 419 (MH^+)). ^{1}H NMR (DMSO-d_6) δ 0.65−0.7 (t, 1H), 0.85−0.9 (t, 2H), 1.35−1.45 (m, 0.7H), 1.5−1.6 (m, 1.3H), 2.05 (s, 1H), 2.25 (s, 2H), 2.35−2.45 (m, 0.7H), 2.55−2.6 (m, 1.3H), 2.9−3.0* (2H), 3.25−3.30* (1H), 3.30−3.35* (1H), 4.5−4.55 (d, 1H), 4.7−4.8 (m, 1H), 4.95−5.05 (d, 1H), 5.25−5.35 (m, 0.65H), 5.4−5.45 (m, 0.35H), 6.65−6.7 (d, 2H), 7.05−7.1 (d, 2H), 7.15−7.4 (m, 4H), 8.0−8.1 (br s, 1H). Verified closely related peaks are rotameric by heating NMR sample to 80 °C, which resulted in the initiation of coalescence of peaks; * peaks were identified based on a COSY experiment (as they were obscured under a large H_2O peak of initial spectra; quantification of related H's is speculated). HRMS calcd for $C_{25}H_{30}N_4O_2$ (MH^+): 419.2447. Found: 419.2447.

(2*S*)-2-Amino-1-[(3*S*)-3-(1*H*-benzoimidazol-2-yl)-3,4-dihydro-1*H*-isoquinolin-2-yl]-3-(4-hydroxy-phenyl)-propan-1-one Trifluoroacetate (1:2) (4f). Starting from **11g**, **4f** was prepared in a similar manner as **4a**. The final crude product isolated from **11g** yielded an isomeric mixture of epimers **4f** and **5c**, based on HPLC and HPLC/MS analysis. By HPLC, desired **4f** proved the front running material (2.78 min), while **5c** ran slightly behind (2.87 min). These compounds were separated by preparative HPLC purification yielding 14% of desired **4f** and 18% of product **5c.** (**4f**: HPLC: 100% at 214 and 254 nm; HPLC/MS: *m*/*z* 413 (MH^+); TLC: 90:9:1 $CHCl_3$:MeOH:NH_4OH R_f = 0.31, homogeneous, also 80:20:5 $CHCl_3$:CH_3OH:HCOOH, R_f = 0.25, homogeneous. ^{1}H NMR (MeOH-d_4) δ 2.2−2.3 (dd, 0.5H), 2.9−3.4 (m, 3.5H), 4.4−4.5 (d, 0.5H), 4.55−4.6 (d, 0.5H), 4.65−5.0 (m, 2H), 5.25−5.3 (t, 0.4H), 5.8−5.9 (t, 0.6H), 6.55−6.6 (d, 1H), 6.75−6.8 (d, 1H), 7.05−7.1 (d, 1H), 7.1−7.65 (m, 8H), 7.7−7.8 (m, 1H). HRMS calc'd for $C_{25}H_{24}N_4O_2$ (MH^+): 413.1978. Found: 413.1965.)

(2*S*)-2-Amino-3-(4-hydroxy-phenyl)-1-[(2*S*)-2-(4-methyl-5-phenyl-1*H*-imidazol-2-yl)-piperidin-1-yl]-propan-1-one Trifluoroacetate (1:2) (4h). Starting from **11b**, **4h** was prepared in a similar manner as **4a** (Yield: 27%; HPLC: 99.7% at 214 and at 254 nm; HPLC/MS: *m*/*z* 405 (MH^+); TLC: 80:20:5 $CHCl_3$:CH_3OH:HCOOH, R_f = 0.35, homogeneous). ^{1}H NMR (MeOH-d_4) δ 0.6−0.7 (m, 0.3H), 1.25−2.35 (m, 5.4 H), 2.4 (s, 1.2H), 2.5 (s, 1.8H), 2.55−2.65 (m, 0.3H), 2.95−3.25 (m, 2H), 3.75−3.85 (d, 0.7H), 4.55−4.95 (m, 2.3H), 5.1−5.15 (t, 0.3H), 6.0−6.05 (t, 0.7H), 6.7−6.75 (d, 1.2H), 6.8−6.85 (d, 0.8H), 7.0−7.05 (d, 1.2H), 7.15−7.2 (d, 0.8H), 7.4−7.65 (m, 5H). HRMS calcd for $C_{24}H_{28}N_4O_2$ (MH^+): 405.2291. Found: 405.2303.

(2*S*)-2-Amino-3-(4-hydroxy-phenyl)-1-[(2*S*)-2-(4-methyl-5-phenyl-1*H*-imidazol-2-yl)-pyrrolidin-1-yl]-propan-1-one Trifluoroacetate (1:2) (4i). Starting from **11c**, **4i** was prepared in a similar manner as **4a** (Yield: 54%; HPLC: 99.4% at 214 and at 254 nm; HPLC/MS: *m*/*z* 391 (MH^+); TLC: 80:20:5 $CHCl_3$:CH_3OH:HCOOH, R_f = 0.08, homogeneous). ^{1}H NMR (MeOH-d_4) δ 2.1−2.35 (m, 3H), 2.5 (s, 3H), 2.5−2.65 (m, 1H), 2.9−3.0 (dd, 1H), 3.15−3.25 (dd, 1H), 3.6−3.7 (m, 1H), 3.9−4.0 (m 1H), 4.45−4.45 (t, 1H), 5.3−5.35 (t, 1H), 6.7−6.75 (d, 2H), 6.95−7.0 (d, 2H), 7.5−7.65 (m, 5H). HRMS calc'd for $C_{23}H_{26}N_4O_2$ (MH^+): 391.2134. Found: 391.2139.

(2*S*)-2-Amino-3-(4-hydroxy-phenyl)-1-[(3*R*)-3-(5-methyl-4-phenyl-1*H*-imidazol-2-yl)-3,4-dihydro-1*H*-isoquinolin-2-yl]-propan-1-one Trifluoroacetate (1:2) (5a). Starting from **14a**, **5a** was prepared in a similar manner as **4a** (Yield: 47%; HPLC: 100% at 214 and 254 nm; HPLC/MS: *m*/*z* 453 (MH^+); TLC: 80:20:5 $CHCl_3$:CH_3OH:HCOOH, R_f = 0.33, homogeneous). ^{1}H NMR (MeOH-d_4) δ 2.35 (s, 3H), 3.1−3.35 (m, 4H), 4.15−4.25 (d, 1H), 4.75−5.0 (m, 2H), 5.75−5.8 (t, 1H), 6.7−6.75 (d, 2H), 7.05−7.1 (d, 2H), 7.15−7.3 (m, 4H), 7.4−7.5 (m, 5H). HRMS calcd for $C_{28}H_{28}N_4O_2$ (MH^+): 453.2290. Found: 453.2281.

(2*S*)-2-Amino-3-(4-hydroxy-phenyl)-1-[(3*R*)-3-(4-methyl-5-propyl-1*H*-imidazol-2-yl)-3,4-dihydro-1*H*-isoquinolin-2-yl]-propan-1-one Trifluoroacetate (1:2) (5b). Starting from **14b**, **5b** was prepared in a similar manner as **4a** (Yield: 56%; HPLC: 100% at 214 and 254 nm; HPLC/MS: *m*/*z* 419 (MH^+); TLC: 80:20:5 $CHCl_3$:CH_3OH:HCOOH, R_f = 0.28, homogeneous). ^{1}H NMR (DMSO-d_6) δ 0.7−0.75 (t, 3H), 1.4−1.5 (m, 2H), 2.1 (s, 3H), 2.4−2.65 (m, 4H), 3.0−3.05 (d, 2H), 4.25−4.3 (d, 1H), 4.65−4.7 (m, 1H), 4.7−4.75 (d, 1H), 5.65−5.7 (t, 1H), 6.7−6.75 (d, 2H), 7.05−7.1 (d, 2H), 7.15−7.3 (m, 4H). HRMS calc'd for $C_{25}H_{30}N_4O_2$ (MH^+): 419.2447. Found: 419.2446.

(2*S*)-2-Amino-1-[(3*R*)-3-(1*H*-benzoimidazol-2-yl)-3,4-dihydro-1*H*-isoquinolin-2-yl]-3-(4-hydroxy-phenyl)-propan-1-one Trifluoroacetate (1:2) (5c). The isolation of this product is described under conditions for **4f**. (**5c**: HPLC: 100% at 214 and 254 nm; HPLC/MS: *m*/*z* 413 (MH^+); TLC: 90:9:1 $CHCl_3$:MeOH:NH_4OH R_f = 0.27. ^{1}H NMR (MeOH-d_4) δ 3.05−3.35 (m, 3H), 3.4−3.5 (dd, 1H), 4.05−4.1 (d, 1H), 4.8−4.85 (d, 1H), 4.85−5.0 (m, 1H), 6.05−6.15 (t, 1H), 6.7−6.75 (d, 2H), 7.1−7.25 (m, 6H), 7.4−7.5 (m, 2H), 7.55−7.65 (m, 2H). HRMS calc'd for $C_{25}H_{24}N_4O_2$ (MH^+): 413.1978. Found: 413.1971.)

Biological Assays. In Vitro Assays. Rat Brain δ and μ Opioid Receptor Binding Assay.[21] Procedure: Male, Wistar rats (150−250 g, VAF, Charles River, Kingston, NY) were sacrificed by cervical dislocation and their brains removed and placed immediately in ice cold Tris HCl buffer (50 mM, pH 7.4). The forebrains were separated from the remainder of the brain by a coronal transection, beginning dorsally at the colliculi and passing ventrally through the midbrain-pontine junction. After dissection, the forebrains were homogenized in Tris buffer in a Teflon-glass homogenizer. The homogenate was diluted to a concentration of 1 g of forebrain tissue per 80 mL Tris and centrifuged at 39 000*g* for 10 min. The pellet was resuspended in the same volume of Tris buffer containing 5 mM $MgCl_2$ with several brief pulses from a Polytron homogenizer. This particulate preparation was used for the δ and μ opioid receptor binding assays. Following incubation with the appropriate peptide ligand [~4 nM [^{3}H]DPDPE for δ and ~0.8 nM [^{3}H]DAMGO for μ] at 25 °C for 2.5 h in a 96-well plate with total volume of 1 mL, the plate contents were filtered through Wallac filtermat B sheets on a Tomtec 96-well harvester. The filters were rinsed three times with 2 mL of 10 mM HEPES (pH7.4), and dried in a microwave oven 1:45 min twice. To each sample area 2 × 40 μL of Betaplate Scint scintillation fluid (LKB) was added and analyzed on a LKB (Wallac) 1205 BetaPlate liquid scintillation counter.

Data Analysis. The data were used to calculate either the % inhibition compared to control binding (when only a single concentration of test compound was evaluated) or a K_i value (when a range of concentrations was tested). % inhibition was calculated as: [(total dpm-test compound dpm)/(total dpm-nonspecific dpm)] × 100. K_d and K_i values were calculated using GraphPad PRISM data analysis program.

[^{35}S]GTPγS Binding Assay in CHO-hγ Cell Membranes.[22] Preparation of Membranes. CHO-hγ cell membranes were purchased from Receptor Biology, Inc. (Baltimore, MD). 10 mg/mL of membrane protein were suspended in 10 mM TRIS-HCl pH 7.2, 2 mM EDTA, and 10% sucrose. Membranes were maintained at 4−8 °C. 1 mL of membranes was added into 15 mL of cold binding assay buffer. The assay buffer contained 50 mM HEPES, pH 7.6, 5 mM $MgCl_2$, 100 mM NaCl, 1 mM DTT, and 1 mM EDTA. The membrane suspension was homogenized with a Polytron two times and centrifuged at 3000 rpm for 10 min. The supernatant was then

centrifuged at 18 000 rpm for 20 min. The pellet was saved in a tube and 10 mL assay buffer was added into the tube. The pellet and buffer were mixed with a Polytron.

Incubation Procedure. The pellet membranes (20 μg/mL) were preincubated with SPA (10 mg/mL) at 25 °C for 45 min in the assay buffer. The SPA (5 mg/mL) coupled with membranes (10 μg/mL) was then incubated with 0.5 nM [^{35}S]GTPγS in the same HEPES buffer containing 50 μM GDP in total volume of 200 μL. Increasing concentrations of receptor agonists were used to stimulate [^{35}S]GTPγS binding. The basal binding was tested in the absence of agonists and no specific binding was tested in the present 10 μM unlabeled GTPγS. The data were analyzed on a Top counter.

DATA analysis: % of basal = (stimulate − nonspecific) × 100/(basal − nonspecific). EC_{50} values were calculated using a GraphPad PRISM data analysis program.

K **Binding and Functional Assays.** Both the κ binding and functional studies were outsourced to Cerep (www.cerep.com). Guinea pig cerebellum was the source for the κ binding study, and rabbit vas deferens tissue was employed for the κ functional study.

In Vivo Assays. Male CD1 mice (18−40 g) were used throughout.

Mouse Abdominal Irritant Test (MAIT).[23] Mice (n = 10) were dosed with the test compound either sc (100 mg/kg at a dosing volume of 10 mL/kg) or icv[24] (10 μg or 100 μg). Following drug treatment, the mice were injected ip with a challenge dose of acetylcholine bromide. The acetylcholine was completely dissolved in distilled water at a concentration of 5.5 mg/kg and injected at the dose of 0.20 mL/20 g. The mice were observed for 10 min for the presence or absence of abdominal constriction response beginning immediately after administration of the acetylcholine. For scoring purposes, an "abdominal constriction" was defined as a contraction of the abdominal musculature accompanied by arching of the back and extension of the limbs. The percent of inhibition of this response was calculated as follows: % inhibition = 100 x (number of nonresponders)/number of animals in group).

Mouse Glass Bead Expulsion Test.[25] A single, colored glass bead (3 mm diameter) was inserted through the anus into the distal colon of nonfasted mice to a distance of approximately 2 cm, with the aid of a small glass rod lubricated with 0.5% methylcellulose. Test compound(s) or vehicle was administered ip (0.1 mL per 10 g body weight) 15 min before bead insertion. After bead insertion, mice were placed in Pyrex animal jars for observation. The time taken to expel the bead from the anus was expressed in minutes for each mouse. Mice with unexpelled beads after 45 min were necropsied to determine bead location. Data presented are mean ± SEM for each group of mice (n = 6−10).

Mouse Fecal Pellet Output Test.[26] Animals were transferred to indirect bedding cages and allowed to acclimate for 24−48 h. Test compound(s) or vehicle was administered ip (0.1 mL per 10 g body weight). The number of fecal pellets expelled was quantified every hour for up to 6 h. Data are presented as cumulative number of pellets over time and have been expressed as mean ± SEM for each group of mice (n = 10). The overall effect of drug treatment was determined by quantifying the area under the curve using the trapezoidal rule.

Data Analysis. Data from the mouse glass bead expulsion test were analyzed by the Kruskal-Wallis Test (nonparametric ANOVA) followed by Dunn's multiple comparisons test. AUCs from the mouse fecal pellet output test were statistically analyzed with a one-way ANOVA followed by the students modified t test with the Bonferroni correction. $P < 0.05$ was considered to be statistically significant in all cases.

Acknowledgment. We appreciate the assistance of William Jones for obtaining HR mass-spectral data and James Gainor for assistance with nomenclature. We also would like to thank John Carson, Patricia Andrade-Gordon, Dennis Hlasta, Scott Dax, Ellen Codd, and Pamela Hornby for fruitful discussions during the course of this work.

Supporting Information Available: Analytical purity data has been tabulated for all targeted compounds. This material is available free of charge via the Internet at http://pubs.acs.org.

References

(1) (a) Fries, D. S. Analgesics. In *Principles of Medicinal Chemistry*, 4th ed.; Foye, W. O., Lemke, T. L., Williams, D. A., Eds.; Willimams and Wilkins: Baltimore, MD, 1995; pp 247−269; (b) Aldrich, J. V. "Analgesics" *Burger's Medicinal Chemistry and Drug Discovery*, 5th ed., Volume 3: Therapeutic Agents, John Wiley & Sons: New York, 1996; pp 321−441.

(2) Riviere, J. M.; Junien, J.-L. Opioid Receptors: Targets for New Gastrointestinal Drug Development. In *Drug Development: Molecular Targets for GI Diseases*; Gaginella, T. S., Guglietta, A., Eds.; Humana Press Inc., Totowa, NJ, pp 203−238.

(3) Hughes, J.; Smith, T. W.; Kosterlitz, H. W.; Fothergill, L. A.; Morgan, B. A.; Morris, H. R. Identification of two related pentapeptides from the brain with potent opiate agonist activity. *Nature (London)* **1975**, *258* (5536), 577−579.

(4) Schiller P. W.; Weltrowska G.; Nguyen T. M.; Wilkes B. C.; Chung N. N.; Lemieux C. TIPP[psi]: a highly potent and stable pseudopeptide delta opioid receptor antagonist with extraordinary delta selectivity. *J. Med. Chem.* **1993**, *36* (21), 3182−3187.

(5) Schiller, P. New Use of Dipeptide Derivatives WO 98/28327, July 2, 1998.

(6) Schiller, P. W.; Nguyen, T. M. D.; Weltrowska, G.; Wilkes, B. C.; Marsden, B. J.; Lemieux, C.; Chung, N. N. Differential stereochemical requirements of μ vs δ opioid receptors for ligand binding and signal transduction: Development of a class of potent and highly δ-selective peptide antagonists. *Proc. Natl. Acad. Sci. U.S.A.* **1992**, *89* (24), 11871−11875.

(7) Marsden, B. J.; Nguyen, T.M−D; Schiller, P. W. Spontaneous degradation via diketopiperazine formation of peptides containing a tetrahydroisoquinoline-3-carboxylic acid residue in the 2-position of the peptide sequence. *Int. J. Pept. Protein Res.* **1993**, *41* (3), 313−316.

(8) Rose, C.; Vargas, F.; Facchinetti, P.; Bourgeat, P.; Bambal, R. B.; Bishop, P. B.; Chan, S. M. T.; Moore, A. N. J.; Ganellin, C. R.; Schwartz, J.-C. Characterization and Inhibition of a Cholecystokinin-Inactivating Serine Peptidase. *Nature* **1996**, *380*, 403−409.

(9) Breslin, H. J.; Miskowski, T. A.; Kukla, M. J.; Leister, W. H.; De Winter, H. L.; Gauthier, D. A.; Somers, M. V. F.; Peeters, D. C. G.; Roevens, P. W. M. Design, Synthesis, and Tripeptidyl Peptidase II Inhibitory Activity of a Novel Series of (S)-2,3-Dihydro-2-(4-alkyl-1*H*-imidazol-2-yl)-1*H*-indoles. *J. Med. Chem.* **2002**, *45* (24), 5303−5310.

(10) von Geldern, T. W.; Hutchins, C.; Kester, J. A.; Wu-Wong, J. R.; Chiou, W.; Dixon, D. B.; Opgenorth, T. J. Azole Endothelin Antagonists. 1. A Receptor Model Explains an Unusual Structure−Activity Profile. *J. Med. Chem.* **1996**, *39*, 957−967.

(11) Gordon, T. D.; Singh, J.; Hansen, P. E.; Morgan, B. A. Synthetic approaches to the 'Azole' peptide mimetics. *TetrahedronLett.* **1993**, 1901−1904.

(12) Byk, G.; Lelievre, Y.; Duchesne, M.; Clerc, F. F.; Scherman, D.; Guitton, J. D. Synthesis and conformational analysis of peptide inhibitors of farnesyltransferase. *Bioorg. Med. Chem.* **1997**, *5* (1), 115−124.

(13) Ross, M. Grimmett *Imidazole and Benzimidazole Synthesis*; Academic Press: San Diego, California; 1997; pp 151−165.

(14) During the course of our work, a couple related benzimidazoles (e.g. **4g**) were reported by Lazarus et al. Compound **4g** was reported possessing high affinity for the δ OR with δ functional antagonist activity (pA_2 7.67), based on the MVD assay. We found **4f** to possess modest agonist activity based on the δ GTPγS OR assay. Balboni, G.; Salvadori, S.; Guerrini, R.; Bianchi, C.; Santagada, V.; Calliendo, G.; Bryant, S. D.; Lazarus, L. H. Opioid pseudopeptides containing heteroaromatic or heteroaliphatic nuclei. *Peptides* **2000**, *21* (11), 1663−1671.

(15) Schiller, P. W.; Nguyen, T. M. D.; Berezowska, I.; Weltrowska, G.; Schmidt, R.; Marsden, B. J.; Wilkes, B. C.; Lemieux, C.; Chung, N. N. The TIPP opioid peptide family: development of a new class of highly potent δ-receptor antagonists with extraordinary δ-selectivity. *Pept. Chem. 1992, Proc. Jpn. Symp., 2nd, 1992, Meeting Date(Pub. 1993)*, 337−340.

(16) Halgren, T. A. Merck molecular force field. *J. Comput. Chem.* **1996**, *17*, 490−642.

(17) Balboni, G.; Salvadori, S.; Guerrini, R.; Negri, L.; Giannini, E.; Jinsmaa, Y.; Bryant, S. D.; Lazarus, L. H. Potent δ-opioid

receptor agonists containing the Dmt-Tic pharmacophore. *J. Med. Chem.* **2002**, *45*, 5556−5563.
(18) Bryant, S. D.; George, C.; Flippen-Anderson, J. L.; Deschamps J. R.; Salvadori, S.; Balboni, G.; Guerrini, R.; Lazarus, L. H. Crystal structure of dipeptides containing the Dmt-Tic pharmacophore. *J. Med. Chem.* **2002**, *45*, 5506−5513.
(19) SYBYL, version 6.8.1, Tripos Inc. (1699 South Hanley Rd., St. Louis, MO 63144).
(20) Guzman, A.; Quintero, C.; Muchowski, J. M. Alkylation of α-*tert*-butoxycarbonylamino ketone enolate anions. A useful synthesis of α-alkyl-α-amino ketones, 2-acylpyrrolidines, and 2-acylpiperidines. *Can. J. Chem.* **1991**, *69* (12), 2059−2063.
(21) Codd, E. E.; Shank, R. P.; Schupsky, J. J.; Raffa, R. B. Serotonin and norepinephrine uptake inhibiting activity of centrally acting analgesics: structural determinants and role in antinociception. *J. Pharmacol. Exp. Ther.* **1995**, *274(3)*, 1263−1270.
(22) Zhang, S.-P.; Wang, H.-Y.; Lovenberg, T. W.; Codd, E. E. Functional studies of bradykinin receptors in Chinese hamster ovary cells stably expressing the human B2 bradykinin receptor. *International Immunopharmacology* **2001**, *1* (5), 955−965.
(23) Collier, H. O.; Dinneen, L. C.; Johnson, C. A.; Schneider, C. The abdominal constriction response and its suppression by analgesic drugs in the mouse. *Br. J. Pharmacol.* **1968**, *32* (2), 295−310.
(24) Haley, T. J.; McCormick, W. G. Pharmacological effects produced by intracerebral injection of drugs in the conscious mouse. *Br. J. Pharmacol.* **1957**, *12*, 12−15.
(25) Rush, B. D.; Ruwart, M. The role of accelerated colonic transit in prostaglandin-induced diarrhea and its inhibition by prostacyclin. *Br. J. Pharmacol.* **1984**, *83*, 157−159.
(26) Coutinho, S. V.; Plotsky, P. M.; Sablad, M.; Miller, J. C.; Zhou, H.; Bayati, A. I.; McRoberts, J. A.; Mayer, E. A. Neonatal maternal separation alters stress-induced responses to viscerosomatic nociceptive stimuli in rat. *Am. J. Physiol. Gastrointest. Liver Physiol.* **2002**, *282* (2), G307−G316.

JM030548R